

PFC/JA-85-15

DIAGNOSIS OF MILDLY RELATIVISTIC ELECTRON
DISTRIBUTIONS BY CYCLOTRON EMISSION

I. H. Hutchinson and K. Kato

Plasma Fusion Center
Massachusetts Institute of Technology
Cambridge, MA 02139

April, 1985

This work was supported by the U.S. Department of Energy Contract No. DE-AC02-78ET51013. Reproduction, translation, publication, use and disposal, in whole or in part by or for the United States government is permitted.

By acceptance of this article, the publisher and/or recipient acknowledges the U.S. Government's right to retain a non-exclusive, royalty-free license in and to any copyright covering this paper.

DIAGNOSIS OF MILDLY RELATIVISTIC ELECTRON
DISTRIBUTIONS BY CYCLOTRON EMISSION

I. H. Hutchinson and K. Kato

Massachusetts Institute of Technology

Plasma Fusion Center

Cambridge, MA 02139

U. S. A.

ABSTRACT

It is shown that electron cyclotron emission can be used for detailed diagnosis of mildly relativistic electron distribution functions, provided the plasma can be viewed along a line of constant magnetic field. Calculations of the emissivity are performed, both for tenuous and finite-density plasmas, whose results allow observations of emission to be deconvolved in terms of the density and anisotropy of the distribution as a function of total electron energy. Prolate distributions require different harmonics, while oblate distributions require different polarizations to be measured. Absorption can also be treated using these results. Some of the issues concerning experimental application are discussed.

1. INTRODUCTION

Mildly relativistic electrons in a magnetic field radiate copiously due to their gyromotion. Expressions for the intensity and polarization of this 'cyclotron' (sometimes called 'synchrotron') emission are readily available [1, 2], in the form of integrals, when the electron velocity distribution function is given. Therefore, in principle at least, it is possible to use observations of the emission characteristics to deduce information about the distribution function, and possibly also the magnetic field when it is unknown.

The way in which this has been done in the past has been to assume some form for the distribution function and then to calculate the emission from it, compare with experiment and then obtain some type of fit. Naturally, the distribution function assumed has a few free parameters which can be adjusted to obtain the fit. It is then these parameters which are said to be 'measured'. For example, one may assume the distribution to be Maxwellian and hence described by two parameters n_e and T_e . This is the basis of the highly successful measurements of electron temperature, T_e , in 'thermal' plasmas via the emission intensity of an optically thick harmonic [3] and of the proposed measurement of electron density, n_e , via an optically thin harmonic [4], the latter not yet fully successful.

When, as is often the case, the electron distribution is not well represented by a Maxwellian, i.e. it is non-thermal, the emission from high energy components can easily dominate over any (presumably) thermal bulk plasma emission. Cyclotron emission thus gives early evidence of deviations from Maxwellian due to high energy 'tails' on the distribution.

Numerous theoretical studies have been made of ways to interpret observations in terms of information about the electron distribution. These studies essentially all adopt a more or less ad hoc model of the distribution with a few free parameters, thus generalizing the Maxwellian approach. Examples of the types of distributions studied include:

1. sums of (shifted) Maxwellians of different energy [5-7];
2. Bimaxwellian distributions [8-10];
3. Maxwellian or Bimaxwellian with 'loss cones' or 'anti loss cones' [11-13].

Naturally, these distributions have been adopted because of a combination of computational ease and a priori ideas of the approximate form of the distribution to be expected. In essence the result of interpretation of an observed spectrum using such a model is a set of 'best-fit' values of the few free parameters, usually a 'density' (or two) a 'temperature' (or two) and an 'anisotropy'. One recognizes that the exact form of the distribution will differ substantially from the model in most cases but nevertheless one has obtained important additional information about the distribution.

The purpose of the present work is to show that, in cases of practical interest, there is the potential for obtaining much more detailed information about the distribution function than is possible via previously adopted approaches. Or, in other words, that one can reasonably expect to be able to fit much more general distribution function models to emission (and possibly absorption) data, thus measuring 'many' parameters of the distribution. To do this type of deconvolution with reasonable accuracy generally requires one to adopt a distribution function model

in which there is a direct, preferably one to one, relationship between the model parameters and the observed spectra.

We show that this can be achieved for reasonably tenuous plasmas (plasma frequency, ω_p , < cyclotron frequency, Ω) provided one can make quantitative measurements along chords through the plasma on which

- (A) the magnetic field is approximately constant in magnitude and at constant angle to the propagation direction;
- (B) the emission from very relativistic electrons ($\gamma \gtrsim 2$) is small.

These criteria are required in order to maintain the one to one correspondence between radiation frequency and a resonant locus in velocity space. If the magnetic field varies strongly, then the emission becomes a volume integral over velocity space and (eventually) the deconvolution becomes impossible. If highly relativistic electrons dominate the emission, then strong cyclotron harmonic overlap will likewise render the deconvolution impossible. (Mild overlap can probably be managed.)

Provided conditions (A) and (B) are satisfied, measurements of the emission intensity (or absorption) spectrum around the first few cyclotron harmonics can provide a continuous (in velocity) parametrization of the distribution function, which can best be expressed as two functions of resonant locus: the number density of particles on the resonant locus, and the anisotropy of the distribution of these electrons (to be defined explicitly later). Such a parametrization can represent rather general distributions with a minimum of ad hoc assumptions about their shape.

Although generalization to other angles is possible, we shall restrict our detailed calculations to perpendicular wave propagation, in which case the resonant locus is a circle, total momentum (p) = constant, and thus the two functions deducible are functions of total electron energy (or momentum).

We develop in Section 2 the formulae for the emissivity and introduce our general model for the electron distribution. In Section 3 we present the results of emissivity calculations for a tenuous plasma. Analytic solutions valid for extreme anisotropy are given in Section 4. In Section 5 we show how the results change when plasma refraction is taken into account, and Section 6 outlines an extension to cyclotron absorption. Some of the conditions necessary for practical application of the technique are mentioned in Section 7.

2. CYCLOTRON EMISSIVITY

Cyclotron emission occurs by interaction of the electromagnetic fields with electrons satisfying the relativistic cyclotron (harmonic) resonance condition:

$$\omega = \ell \frac{\Omega}{\gamma} + k_{\parallel} v_{\parallel} = \frac{\Omega}{(1+p^2)^{1/2}} \left[\ell + \frac{\omega}{\Omega} N_{\parallel} p_{\parallel} \right] \quad (1)$$

where ω is the wave frequency, \vec{k} its k-vector, \vec{N} the refractive index vector ($\vec{k}c/\omega$), Ω the cyclotron frequency (eB/m_e), ℓ the harmonic number, γ the relativistic mass increase factor and \vec{p} the relativistic electron momentum in units of $m_e c$ (so that $\gamma^2 = 1 + p^2$). We shall refer to components parallel and perpendicular to \vec{B} by \parallel and \perp . For given frequency and N_{\parallel} this resonance defines an ellipse in momentum space

which may be written

$$\frac{(p_{\parallel}-d)^2}{a^2} + \frac{p_{\perp}^2}{b^2} = 1 \quad (2)$$

where

$$\begin{aligned} a^2 &= [\ell^2 \Omega^2 / \omega^2 (1 - N_{\parallel}^2) - 1] / (1 - N_{\parallel}^2) \\ b^2 &= [\ell^2 \Omega^2 / \omega^2 (1 - N_{\parallel}^2) - 1] \\ d &= \ell \Omega N_{\parallel} / \omega (1 - N_{\parallel}^2) \end{aligned} \quad (3)$$

The cyclotron emissivity of a plasma is then given by an integral of the distribution function, weighted by the single particle emissivity, over this ellipse. Therefore emissivity at a given ω/Ω , ℓ and N_{\parallel} is related only to particles on this ellipse. As we shall see, it will be convenient to represent the distribution in terms which recognize this relationship.

We shall in fact choose to analyze here only the perpendicular propagation case, $N_{\parallel} = 0$. As justification for this specialization we cite, in addition to its simplification of the analysis, that this choice minimizes harmonic overlap and also corresponds to the case most likely to be of experimental interest. A notable drawback to this choice is that its symmetry makes it impossible to distinguish positive and negative p_{\parallel} . Thus reflectional symmetry or asymmetry in the plane $p_{\parallel} = 0$ is left undetermined.

For perpendicular propagation the (spontaneous) cyclotron emission coefficient can be written [2]

$$j_{\ell}(\omega) = \frac{e^2 \omega^2}{8\pi^2 \epsilon_0 c} N_{\pm} \int \left\{ \begin{array}{l} p_{\parallel} J_{\ell} \\ N_{-} K J_{\ell} \gamma + p_{\perp} J'_{\ell} \end{array} \right\}^2 \frac{1}{\gamma^2} \delta\left(\omega - \frac{\ell \Omega}{\gamma}\right) f(\vec{p}) d^3 p \quad (4)$$

where upper and lower signs and terms correspond to ordinary and extraordinary modes respectively; the argument of the Bessel functions, J_ℓ , is $\ell N_\pm p_\perp / \gamma$; f is the unnormalized \vec{p} -distribution function and

$$K \equiv \frac{\omega_p^2 \Omega \omega}{(\omega^2 - \omega_p^2)^2 - \Omega^2 \omega^2} \quad (5)$$

In this formula the delta function restricts the integral to the circular resonance and the implicit assumption is that the wave properties (N and polarization) are determined by some 'bulk' cold plasma through which the resonant locus in momentum space does not pass. In other words, it is valid at frequencies other than the thermal cyclotron resonances, $\omega = \ell \Omega$. In the tenuous plasma case, $N_\pm \rightarrow 1$, $K \rightarrow 0$, j_ℓ becomes the well known Schott-Trubnikov formula [1] (more often written in terms of $\vec{\beta} = \vec{v}/c$ rather than \vec{p}). The total emissivity is a sum over all ℓ but if there is no harmonic overlap we can treat harmonics separately.

Taking the distribution function to be gyrotropic ($f = f(p_\perp, p_\parallel)$) the integral becomes:

$$j_\ell(\omega) = \frac{e^2 \omega}{8 \pi^2 \epsilon_0 c} N_\pm 2 \pi p^3 \int_0^\pi \left\{ N_{-K}(\gamma/p) J_\ell + \sin \theta J'_\ell \right\}^2 f \sin \theta d\theta \quad (6)$$

over the sphere $p = [\gamma^2 - 1]^{1/2} = [(\ell \Omega / \omega)^2 - 1]^{1/2}$. Here θ is the pitch angle, $p_\parallel / p = \cos \theta$. With the emissivity in this form it is plain that the natural way to express the distribution function is in the form of a product:

$$f(\vec{p}) = f_p(p) f_\theta(p, \theta) \quad (7)$$

where $f_p(p)$ contains the variation with p of the total number of particles on the sphere and $f_\theta(p, \theta)$ gives the anisotropy of f at a given p . That is

$$4\pi p^2 f_p(p) = \int_0^\pi f(\vec{p}) 2\pi p^2 \sin\theta d\theta \quad (8)$$

$$f_\theta(p, \theta) = f(\vec{p})/f_p(p); \quad \int_0^\pi f_\theta(p, \theta) \sin\theta d\theta = 2 \quad (9)$$

In this case

$$j_\ell = \frac{e^2 N_\pm}{8\pi^2 \epsilon_0 c} \left(\frac{\ell \Omega}{\gamma} \right) 2\pi p^3 f_p(p) \int_0^\pi \left\{ \begin{array}{l} \cos\theta J_\ell \\ N_{-K}(\gamma/p) J_\ell + \sin\theta J'_\ell \end{array} \right\}^2 f_\theta \sin\theta d\theta \quad (10)$$

If the distribution function is isotropic, $f_\theta = 1$, a measurement of j_ℓ from a single harmonic is sufficient to give $f_p(p)$ and hence the whole distribution function, since the angle integrals are simply numbers independent of f_p . Of more interest is the situation where f is not isotropic. Then a measurement of j_ℓ at a single harmonic is insufficient to determine the angular dependence of f_θ . However, if j_ℓ is available for two different harmonics then their ratio is independent of f_p but depends on f_θ through the pitch angle integrals. The problem is thus reduced to an investigation of how the anisotropy of the distribution affects the pitch angle integrals:

$$\Theta_\ell^\pm(p) \equiv \int_0^\pi \left\{ \begin{array}{l} \cos\theta J_\ell(x_\pm \sin\theta) \\ N_{-K}(\gamma/p) J_\ell(x_\pm \sin\theta) + \sin\theta J'_\ell(x_\pm \sin\theta) \end{array} \right\}^2 f_\theta \sin\theta d\theta \quad (11)$$

where $x_\pm = \ell N_\pm p / \gamma$.

In general we shall have only a very few independent harmonics, since for large l , overlap becomes more and more severe. Therefore, we are obliged now to make our only ad hoc assumption, namely that we shall choose f_θ to have a form parametrized by a single function of p . Explicitly we take

$$f_\theta = L \exp(-\Lambda(p) \cos^2 \theta), \quad (12)$$

where [14]

$$L = 2 \sqrt{\frac{\Lambda}{\pi}} \frac{1}{\operatorname{erf}(\sqrt{\Lambda})} \quad (13)$$

is chosen to satisfy the normalization condition $\int_0^\pi f_\theta \sin \theta \, d\theta = 2$. Of course, other choices of function are possible but this form is well suited to representing distributions which are reasonably smooth and either prolate (enhanced in the parallel direction) or oblate (enhanced in the perpendicular direction) corresponding to Λ less or greater than zero respectively. The form is illustrated in Fig.1. This form cannot represent distributions with maxima or minima at angles other than $\theta = 0$ or $\pi/2$. If this were required then, in principle, our results could be used in a direct generalization utilizing a sum of two functions of the above form. This would naturally require more information to determine the appropriate sum. Distributions which are asymmetric in p_\parallel may be dealt with only by assumptions about this asymmetry since no information comes from the emission. For example it might be appropriate to take f_θ non zero only for $\theta < \pi/2$. Such a case is easily treated using the results here given, but to avoid confusion we shall deal with symmetric distributions and present results for cases where Eq.(12) applies for the full range of θ , 0 to π .

With this choice of f_θ distribution we can calculate the pitch angle integrals as a function of the anisotropy factor, Λ , and momentum. Using the values of these integrals the deconvolution from observations can be performed to give $f_p(p)$ and $\Lambda(p)$ and hence the distribution.

3. TENUOUS PLASMA, IGNORING REFRACTIVE EFFECTS

We now restrict our attention to cases in which the finite plasma density effects can be ignored, generally requiring $\omega \gg \omega_p$. Later it will be shown how to correct these results when the finite density is not ignorable. For the present, then, the angle integrals are

$$\Theta_\ell^\pm(p, \Lambda) = 2 \int_0^{\pi/2} \left\{ \begin{array}{l} \cos \theta J_\ell(x \sin \theta) \\ \sin \theta J'_\ell(x \sin \theta) \end{array} \right\}^2 L \exp(-\Lambda \cos^2 \theta) \sin \theta d\theta \quad (14)$$

with $x = \ell p / \gamma (= \ell v / c)$. For general values of Λ we must now resort to numerical computation of these angle integrals. The results are shown in Figs 2 through 5 in which we plot the value of Θ as a function of Λ for a range of electron energy values at the first four cyclotron harmonics. Energies greater than $\gamma = \ell / (\ell - 1)$ for $\ell > 1$ will overlap with a lower harmonic adding complexity to the deconvolution process. For example, above 511 keV the second harmonic overlaps the first.

In order to deduce the effective value of Λ requires one to take a ratio of emissivities so as to eliminate $f_p(p)$. Such a ratio can be obtained from the Θ data. As examples of particular interest we show in Fig.6 the ratio j_3/j_2 as a function of Λ and in Fig.7 the ratio j_2^+/j_2^- . These show that the harmonic ratio j_3/j_2 is a sensitive measure of Λ for $\Lambda < 0$, prolate distributions, while the polarization ratio j_2^+/j_2^- is a sensitive measure of Λ for $\Lambda > 0$, oblate distributions.

The insensitivity of these ratios for the opposite inequalities prevents them being useful for those cases. For example the j_3/j_2 ratio cannot be used effectively to diagnose $\Lambda > 0$, oblate anisotropies.

The general procedure is to deduce $\Lambda(p)$ from a suitable ratio of emissivities, using, for example,

$$\frac{j_3 \left(\frac{3\Omega}{\gamma} \right)}{j_2 \left(\frac{2\Omega}{\gamma} \right)} = \frac{3 \theta_3(\Lambda, p)}{2 \theta_2(\Lambda, p)} \quad (15)$$

With this in hand $f_p(p)$ can be deduced from the emissivity by using

$$j_\ell \left(\frac{\ell\Omega}{\gamma} \right) = \frac{e^2}{8\pi^2 \epsilon_0 c} \frac{\ell\Omega}{\gamma} 2\pi p^3 f_p(p) \theta_\ell(\Lambda, p). \quad (16)$$

4. EXTREME ANISOTROPY: ANALYTIC APPROXIMATIONS

It is useful and revealing to obtain analytic approximations valid in two opposite limits.

4.1. Parallel Tail , $-\Lambda \gg 1$

In this case, where the distribution is confined to a narrow 'cigar shaped' region along the p_{\parallel} axis we can make the approximations $\sin\theta \approx \theta$, $\cos^2\theta \approx (1-\theta^2)$, $J_\ell \approx (x\theta/2)^\ell/\ell!$ and thus

$$f_\theta \approx 2(-\Lambda) \exp(\Lambda\theta^2) \quad -\Lambda \gg 1 \quad (17)$$

$$\theta_\ell^\pm \approx 2 \int_0^\infty \left\{ \frac{(x\theta/2)^\ell/\ell!}{\ell(x\theta/2)^\ell/x\ell!} \right\}^2 (-\Lambda) \exp(\Lambda\theta^2) 2\theta d\theta \quad (18)$$

The integral may now be evaluated to give

$$\Theta_{\ell}^{\pm} \approx \frac{2}{(-\Lambda)^{\ell} \ell!} \left(\frac{p \ell}{2\gamma} \right)^{2\ell} \left\{ \frac{1}{\gamma^2/p^2} \right\} \quad (19)$$

Notice that the integral is now effectively over a short vertical straight line segment on which $f \propto \exp(\Lambda p_{\perp}^2/p^2)$. Therefore this limit models a distribution with Gaussian perpendicular variation corresponding to a perpendicular temperature

$$T_{\perp} = \frac{m_0 c^2}{-\Lambda} \frac{p^2}{2\gamma} \quad (20)$$

In this limit of narrow perpendicular spread, when the integral can be taken as a straight line, it is easy to show that the emissivity of the ℓ^{th} harmonic is proportional to the $2\ell^{\text{th}}$ moment of the perpendicular momentum,

$$j_{\ell}^{\pm} \approx \frac{e^2 \omega}{8\pi^2 \epsilon_0 c} \frac{2}{p} \left(\frac{\ell}{2\gamma} \right)^{2\ell} \frac{1}{\ell!^2} \left\{ \frac{p^2}{\gamma^2} \right\} \int_0^{\infty} f(\vec{p}) p_{\perp}^{2\ell} 2\pi p_{\perp} dp_{\perp} \quad (21)$$

regardless of whether the perpendicular variation of f is Gaussian, as our model assumes, or not [15]. In the absence of indications to the contrary the Gaussian assumption seems most natural and then the ratio of harmonic emissivities gives directly the perpendicular 'temperature'. It should be noted, however, that using the 'straight line' approximation Eq.(21) rather than the full pitch angle integral for a case where $f_p \approx \text{constant}$ and $p \ll \gamma$ leads to an overestimate of Θ by a factor of approximately

$$\left(1 + \frac{2\ell + 1}{-2\Lambda} \right)^{\left\{ \begin{matrix} \ell \\ \ell-1 \end{matrix} \right\}} \quad (22)$$

Thus, for example, the value of T_{\perp} deduced from the j_3/j_2 ratio using the 'straight line' approximation is an overestimate by already 25% when $\Lambda \approx -20$. This approximation is thus accurate only for extremely anisotropic distributions.

4.2. Perpendicular 'tail', $\Lambda \gg 1$

When $\Lambda \gg 1$ the electron distribution is restricted to a 'disc' near the p_{\perp} axis. We may therefore approximate $\sin\theta = 1$, $\cos\theta = \pi/2 - \theta = \phi$ so that

$$f_{\theta} \approx 2 \sqrt{\frac{\Lambda}{\pi}} \exp[-\Lambda(\pi/2 - \theta)^2] \quad (23)$$

$$\Theta_{\ell}^{\pm} \approx \left\{ \frac{J_{\ell}^2(x)}{J_{\ell}^{\prime 2}(x)} \right\}_{-\infty}^{\infty} \left\{ \frac{\phi^2}{1} \right\} 2 \sqrt{\frac{\Lambda}{\pi}} \exp(-\Lambda\phi^2) d\phi \quad (24)$$

and hence

$$\Theta_{\ell}^{\pm} \approx \left\{ \frac{J_{\ell}^2(x)/\Lambda}{2J_{\ell}^{\prime 2}(x)} \right\} \quad (25)$$

In this case the approximately straight line segment to which the integral is restricted is horizontal and $f \propto \exp(-\Lambda p_{\parallel}^2/p^2)$ modelling a distribution with Gaussian parallel variation and parallel temperature

$$T_{\parallel} = \frac{m_0 c^2}{\Lambda} \frac{p^2}{2\gamma} \quad (26)$$

The emissivity is in fact a simple moment of the parallel momentum, again regardless of the precise form of model for the distribution,

$$j_{\ell}^{\pm}(\omega) = \frac{e^2 \omega}{8\pi^2 \epsilon_0 c} \left\{ \begin{matrix} J_{\ell}^2(x) \\ J_{\ell}^{\prime 2}(x) \end{matrix} \right\} 2\pi p \int_{-\infty}^{\infty} f(\vec{p}) \left\{ \begin{matrix} p_{\parallel}^2 \\ p^2 \end{matrix} \right\} dp_{\parallel} \quad (27)$$

where $x = \ell p / \gamma$, and of course $\omega = \ell \Omega / \gamma$. The polarization ratio thus provides a direct measurement of the second moment of p_{\parallel} and hence the 'mean parallel energy'

$$T_{\parallel} \equiv \frac{m_0 c^2}{\gamma} \frac{\int p_{\parallel}^2 f(\vec{p}) dp_{\parallel}}{\int f(\vec{p}) dp_{\parallel}} = \frac{m_0 c^2 p^2 J_{\ell}^{\prime 2}(x) j_{\ell}^+}{\gamma J_{\ell}^2(x) j_{\ell}^-} \quad (28)$$

These approximations, valid for highly anisotropic distributions, are useful for understanding the results already observed in the numerical curves for $|\Lambda| \gg 1$. However, it is likely that most experimental plasmas will be insufficiently anisotropic for these to be accurate approximations. Usually the numerical results will be required. This point is illustrated in Fig.8 where the approximate and exact results are compared.

5. FINITE-DENSITY CORRECTIONS

When the plasma density is such that significant modifications to the refractive index occur, the full Eq.(6) for the emissivity must be used. The values of the refractive index for perpendicular propagation are

$$N_{+} = 1 - \frac{\omega_p^2}{\omega^2} \quad ; \quad N_{-} = 1 - \frac{\omega_p^2 (\omega^2 - \omega_p^2)}{\omega^2 (\omega^2 - \omega_p^2 - \Omega^2)} \quad (29)$$

The corrections are of three basic types. First, the argument of the Bessel function ($\ell k_{\perp} v_{\perp} / \omega$) is altered by the additional factor N_{\pm} because

k_{\perp} is different. Second, the emissivity is enhanced by the factor N_{\pm} (again basically because of phase speed modification). Third, for the extraordinary mode, since K is no longer zero, an extra term must be included in the pitch angle integral. This correction arises because of modification of the wave polarization.

The ordinary wave, whose polarization is unchanged at perpendicular propagation, has no correction of the third type. Therefore our previous results for the angle integrals can be used directly. All that is required is to use $N_{\perp p}$ instead of p inside the integral. Then an additional multiplication by N_{\pm} corrects j^+ completely. Note that the correction factors will be different for different harmonics so that Fig.6 cannot be used directly. Generally the effect will be to reduce the lower harmonics relatively more than the higher compared to tenuous plasma calculations; thus for example j_3^+/j_2^+ is increased by finite density effects.

The extraordinary mode is much more difficult to deal with exactly. To do so would require a calculation of the angle integral for essentially every desired value of ω_p/Ω . However, provided we exclude frequencies close to a wave resonance ($N \rightarrow \infty$), which in any case will tend not to be easy to deal with experimentally, we can employ an approximate correction scheme which enables us to use the angle integrals already evaluated.

The approach is to note that K is already a small correction and the recurrence formulae for Bessel functions give

$$J_{\ell}(\ell N_{\perp} \sin \theta / \gamma) = \frac{N_{\perp} \sin \theta}{\gamma} (J_{\ell}^{\prime} + J_{\ell+1}) \quad (30)$$

(all the arguments being the same). The $J_{\ell+1}$ term may also be treated as small, provided $N_p \sin \theta / \gamma < 1$. Therefore the finite density correction term inside the integral can be written as $N^2 K (1 + J_{\ell+1} / J_{\ell}')$ times a term of the same form as the tenuous plasma term; i. e. $\sin \theta J_{\ell}'$. Although $J_{\ell+1} / J_{\ell}'$ is a function of θ , it represents only a second order correction, so we shall obtain sufficient accuracy if we treat it as a constant, equal to its value at the angle at which the integrand is maximum. This angle may readily be shown to be given by

$$\begin{aligned} \sin^2 \theta_{\max} &= \frac{\ell}{-\Lambda} \quad \text{for } -\Lambda > \ell \\ &= 1 \quad \text{otherwise.} \end{aligned} \tag{31}$$

Therefore the approximate form we obtain for the finite density angle integral then reduces (using the expansion for the Bessel functions) to

$$\Theta^-(p) \approx \left[1 + N^2 K \left\{ 1 + \frac{N_p^2}{2\gamma^2} \frac{\ell}{\ell+1} \sin^2 \theta_{\max} \right\} \right]^2 \Theta_{\text{tenuous}}^-(N_p). \tag{32}$$

This approximate form introduces an error of less than $\sim 10\%$ in the coefficient of K , for $N_p / \gamma < 1$. And it becomes exact in the limit $p_{\perp} \rightarrow 0$, (i.e. $\Lambda \rightarrow -\infty$ or $p \rightarrow 0$).

In Fig.9 we plot values of $\Theta_{\ell}^{\pm} (p^3 \omega / N_{\pm}^2 \Omega)$ as a function of ω showing how the finite plasma corrections alter the emissivity. The approximate treatment of the extraordinary mode is indistinguishable in the figure from the full angle integration of the exact equations. The purpose of plotting this particular quantity is that it is a normalized form of the radiation source function, j / N_r^2 (see Section 7); i.e.

$$\frac{\Theta_{\pm}^3 \omega}{N_{\pm}^2 \Omega} = \left(\frac{4\pi\epsilon_0 c}{e^2} \right) \frac{1}{f_p \Omega} \frac{j_l}{N_{\pm}^2} \quad (33)$$

Thus it takes the shape of the emission spectrum from a plasma in which $f_p = \text{constant}$. We have cut off each harmonic at the point where it would overlap with the next lower harmonic, so as to avoid confusion. Naturally, if f_p extends to high enough energy in a practical situation overlap will occur. We have also suppressed emission between Ω and the upper hybrid frequency, $(\omega_p^2 + \Omega^2)^{1/2}$, for clarity and also because it will tend to be inaccessible.

6. ABSORPTION

It may also be of interest to use cyclotron absorption caused by non-thermal electrons for diagnosis of the distribution function. The absorption coefficient, α , may be deduced immediately in integral form from the emission coefficient using the principle of detailed balance [1]. It is obtained, for the case of perpendicular propagation, by replacing $f(p)$ in the equation for j Eq.(6) by

$$- \frac{8\pi^3 \gamma}{N_r^2 \omega^2 m_e} \frac{1}{p_{\perp}} \frac{\partial f}{\partial p_{\perp}^2} \quad (34)$$

where N_r is the ray refractive index and is equal to the wave refractive index N_{\pm} for perpendicular propagation.

This simple relationship enables us to use our results to deduce the perpendicular derivative $\partial f / \partial p_{\perp}^2$ from measurements of absorption provided we regard it as being represented by the form

$$\frac{\partial f}{\partial p_{\perp}^2} = \left(\frac{\partial f}{\partial p_{\perp}^2} \right)_p L \exp(-\Lambda \cos^2 \theta). \quad (35)$$

However, this is a different form of assumption about f itself than was made for emission. That previous form Eq.(12) would have led to

$$2 \frac{\partial f}{\partial p_{\perp}^2} = \frac{1}{p} \left(\frac{\partial f}{\partial p} + \frac{\cot \theta}{p} \frac{\partial f}{\partial \theta} \right) = \frac{1}{p} \left(\frac{\partial f_p}{\partial p} f_{\theta} + \frac{\Lambda \cos^2 \theta}{p} f_p f_{\theta} \right) \quad (36)$$

combining both f_p and $\partial f_p / \partial p$. This is not immediately amenable to the approach we have adopted. Therefore combinations of measurements of j and α are not directly interpretable by the present methods in general.

An exception to this difficulty is the extremely anisotropic case $-\Lambda \gg 1$. For this parallel tail type, one may readily show that the absorption coefficient reduces to a moment of the perpendicular momentum (regardless of the exact angular dependence):

$$\alpha_{\ell}^{\pm} = \frac{2e^2 \pi}{m_e \epsilon_0 c} \frac{\gamma}{p} \left(\frac{\ell}{2\gamma} \right)^{2\ell} \frac{2\ell}{\ell!^2} \left\{ \begin{matrix} p \\ \gamma \end{matrix} \right\} \int_0^{\infty} f(\vec{p}) p_{\perp}^{2(\ell-1)} 2\pi p_{\perp} dp_{\perp} \quad (37)$$

just as with the emission Eq.(21) (though the order of the moment is 2 less). In particular j_{ℓ} / α_{ℓ} reduces to the anticipated Rayleigh-Jeans type of Black Body value, $\omega^2 T_{\perp} / 8\pi^3 c^2$ in a tenuous plasma, giving the perpendicular temperature. This simplification occurs in the vertical straight line approximation because integration by parts is possible. In other cases no such simplification is available.

7. PRACTICAL APPLICATION

The application of our results to a practical situation requires primarily that measurements of emission intensity should be able to be related to the emissivity and hence to the distribution function.

Naturally a view of the plasma will provide only an average value of j along the line of sight. This is, of course, no different from many other types of diagnostic and radial information may be obtained, in principle, by Abel inversion etc. More importantly the plasma view must be sufficiently collimated that the propagation is truly perpendicular. This requires that the spread of resonant loci in p -space arising from the angular spread in view (via Eq.(2)) be much smaller than the typical spread of $f(\vec{p})$. For relativistic particles this is not an overly stringent condition.

For the emission intensity to be proportional to j also requires that absorption be negligible i.e. the plasma must be optically thin. This will depend on $f(\vec{p})$ but may, in some circumstances rule out the first harmonic [16] or ultimately prevent the approach from working for any harmonic. For example the thermal bulk plasma is usually too dense even up to $\ell = 3$ to be diagnosed explicitly therefore one must avoid $\omega = \ell\Omega$ in the spectrum.

When the plasma refraction is non-negligible, it is important also to account for this fact in relating the observed intensity to local emissivity. If absorption is negligible then the intensity is given by [1],

$$I = \int \frac{j}{N_r^2} d\ell \quad (38)$$

where N_r is the ray refractive index (again equal to N for perpendicular propagation). This corrects for the fact that solid angles within which the radiation propagates vary with N_r . It was in anticipation of this point that Fig.9 plotted the quantity in Eq.(33) which is the appropriately normalized source function observed by emission measurements in finite-density plasmas.

In practice, another difficulty may be harmonic overlap which will tend to obscure the true harmonic ratios. Mild overlap may be able to be compensated for using information from more than two harmonics or else by making plausible assumptions about how the distribution function extrapolates. However, strongly relativistic electron distributions will probably defeat our scheme.

A final critical practical point is the necessity of avoiding radiation entering the acceptance angle by multiple reflections from the chamber walls. This effect would tend to distort as well as enhance the spectrum because the multiply reflected radiation will not in general propagate perpendicular to the field nor along the initial line of sight where $|B|$ is constant. Rather effective viewing dumps are required in order to reduce the multiple reflections to a negligible level and despite the fact that suitable ones have been developed [17] this problem will probably remain the limiting factor in practical experiments. This is particularly so for large anisotropy where one wishes to take the ratio of two emissivities (either harmonics or polarizations) with very different magnitudes.

8. CONCLUSION

We have shown that cyclotron emission from mildly relativistic electrons can potentially provide very detailed information about the electron distribution function. We have calculated emissivities for tenuous and finite-density plasmas using a model of the distribution which lends itself to direct determination via the cyclotron emission. Using these calculations it is possible to determine directly the anisotropy and the phase space density as a function of total electron energy from measurements of two distinct optically thin harmonics (or polarizations). These results promise to be directly applicable to diagnosing plasmas with significant 'tails' on the electron distribution due, for example, to RF heating or current drive or simple electron run-away.

ACKNOWLEDGEMENTS

This work was supported under U. S. Department of Energy contract #DE-AC02-78ET51013.

REFERENCES

- [1] BEKEFI, G., 'Radiation Processes in Plasmas' Wiley, New York (1966).
- [2] FREUND, H. P., WU, C. S., Phys. Fluids, 20 (1977) 963.
- [3] e.g. HUTCHINSON, I. H., Infrared Phys., 18 (1978) 763.
- [4] ENGLEMAN, F., CURATOLO, M., Nucl. Fusion, 13 (1973) 497.
- [5] CELATA, C. M., BOYD D. A., Nucl. Fusion, 17 (1977) 735.
- [6] TAMOR, S., Nucl. Fusion, 19 (1979) 455.
- [7] FIDONE, I., GRANATA, G., MEYER, R. L., JORNADA, E. H., SCHNEIDER, R. S., ZIEBELL, L. F., Phys. Fluids, 23 (1980) 1336.
- [8] LIU, C. S., MOK, Y., Phys. Rev. Lett., 38 (1977) 162.
- [9] FREUND, H. P., WU, C. S., LEE, L. C., DILLENBERG, D., Phys. Fluids, 21 (1978) 1502.
- [10] FIDONE, I., GRANATA, G., MEYER, R. L., Plasma Phys., 22 (1980) 261.
- [11] WINSKE, D., PETER, Th., BOYD, D. A., Phys. Fluids, 26 (1983) 3497.
- [12] FREUND, H. P., WU, C. S., GAFFEY, J. D., Phys. Fluids, 27 (1984) 1396.
- [13] CELATA, C. M., Nucl. Fusion, 25 (1985) 35.
- [14] Error function of imaginary argument (for $\lambda < 0$) is to be interpreted, via the defining integral, as a 'Dawson' function.
- [15] GIRUZZI, G., FIDONE, I., GRANATA, G., MEYER, R. L., Phys. Fluids, 27 (1984) 1704.
- [16] MAZZUCATO, E., EFTHIMION, P., FIDONE, I., Relativistic Effects on Cyclotron Wave Absorption by an Energetic Electron Tail in the PLT Tokamak, Princeton University Report PPPL-2122 (1984).
- [17] KATO, K., HUTCHINSON, I. H., Design and Performance of Compact Submillimeter Beam Dumps, M.I.T. Report PFC/RR-84-11 (1984).

FIGURE CAPTIONS

- Figure 1 The pitch-angle distribution, f_{θ} , versus the momentum pitch-angle, θ , for representative values of the anisotropy factor, Λ .
- Figure 2 The first harmonic cyclotron emission pitch-angle integral, Θ_1 , versus the anisotropy factor, Λ , for (a) ordinary mode, (b) extraordinary mode. The different curves correspond to different total electron energy (in keV) as indicated on the figure.
- Figure 3 As for Figure 2 but for the second harmonic.
- Figure 4 As for Figure 2 but for the third harmonic.
- Figure 5 As for Figure 2 but for the fourth harmonic.
- Figure 6 The harmonic ratio, j_3/j_2 , versus the anisotropy factor, Λ , for different values of the total electron energy; (a) ordinary mode, (b) extraordinary mode.
- Figure 7 Polarization ratio of the second harmonic emission, j^+/j^- , versus the anisotropy factor, Λ , for different values of the total electron energy.
- Figure 8 Approximations to the second harmonic cyclotron emission pitch-angle integral, Θ_2 , versus the anisotropy factor, Λ , for (a) ordinary mode, (b) extraordinary mode. For $|\Lambda| \gg 1$ these approximations agree well with the exact solutions, shown by the broken lines.

Figure 9 Normalized emissivity, $\theta_{\mu} p^3 \omega / N^2 \Omega$, versus the normalized frequency, ω / Ω , for the first three harmonics with $\Lambda = 0$, at three densities: $\omega_p^2 / \Omega = 0, 0.25, 0.5$. Harmonic overlap is suppressed. (a) Ordinary mode; (b) Extraordinary mode.

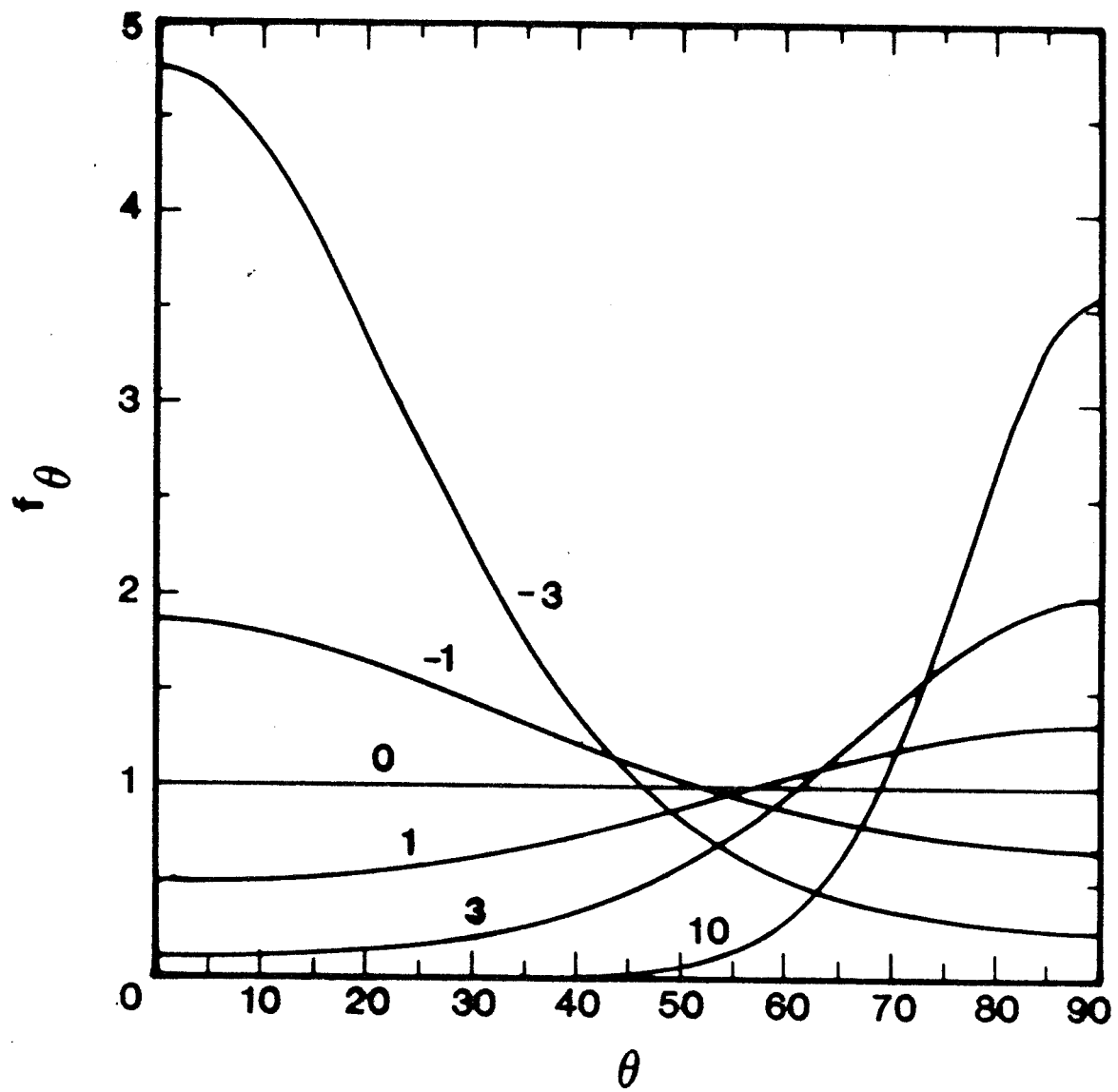


Figure 1

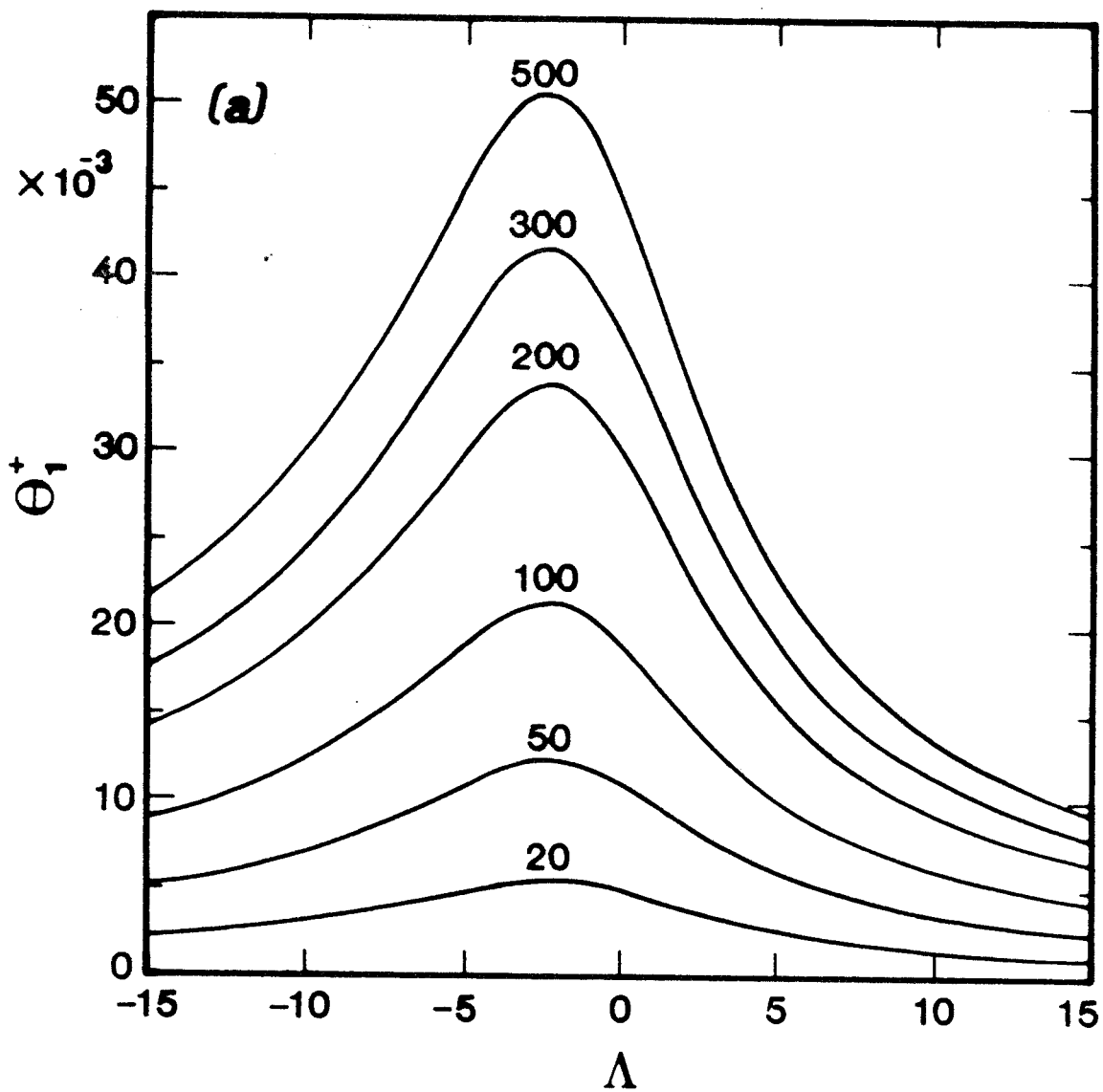


Figure 2 (a)

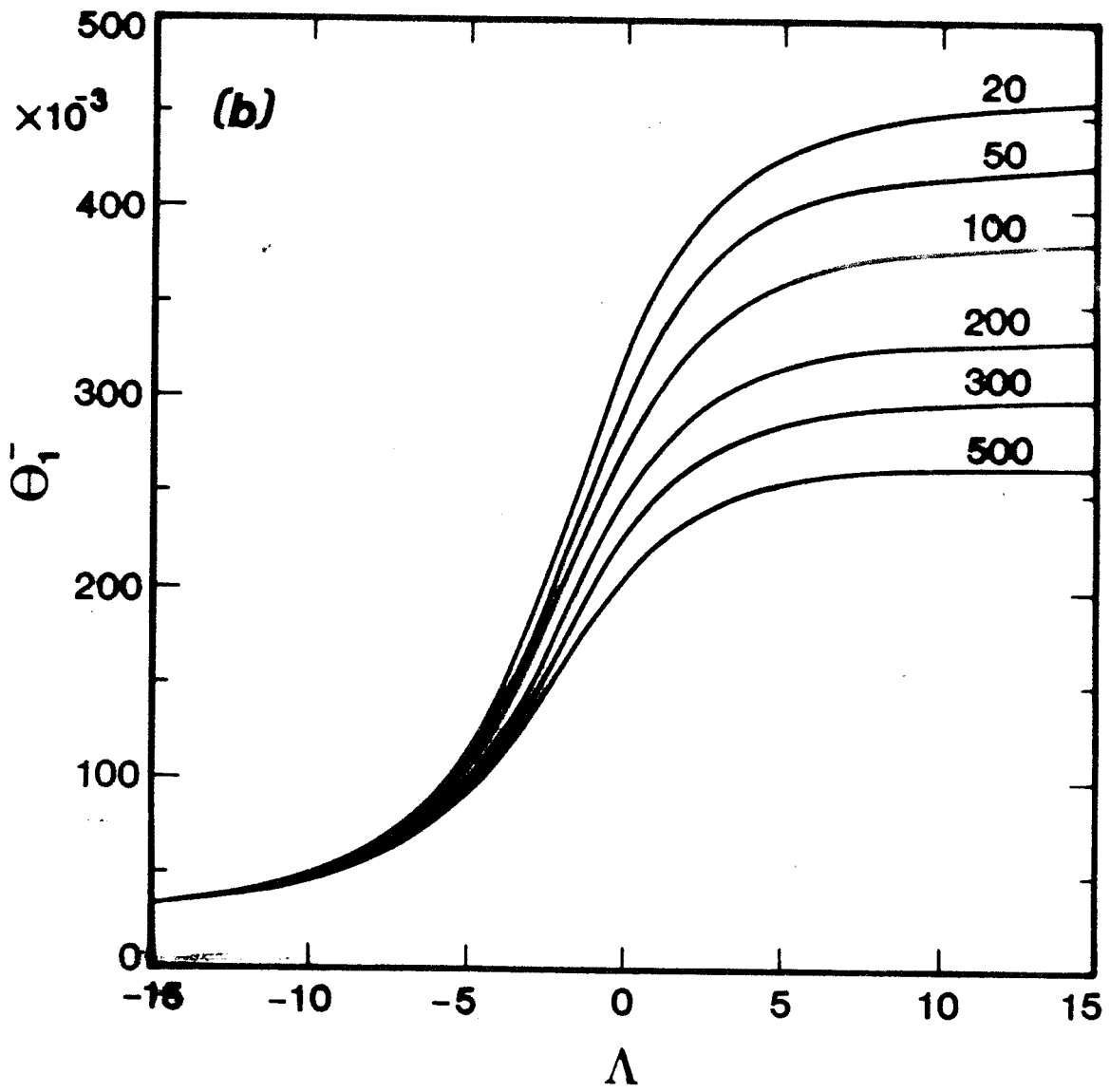


Figure 2 (b)

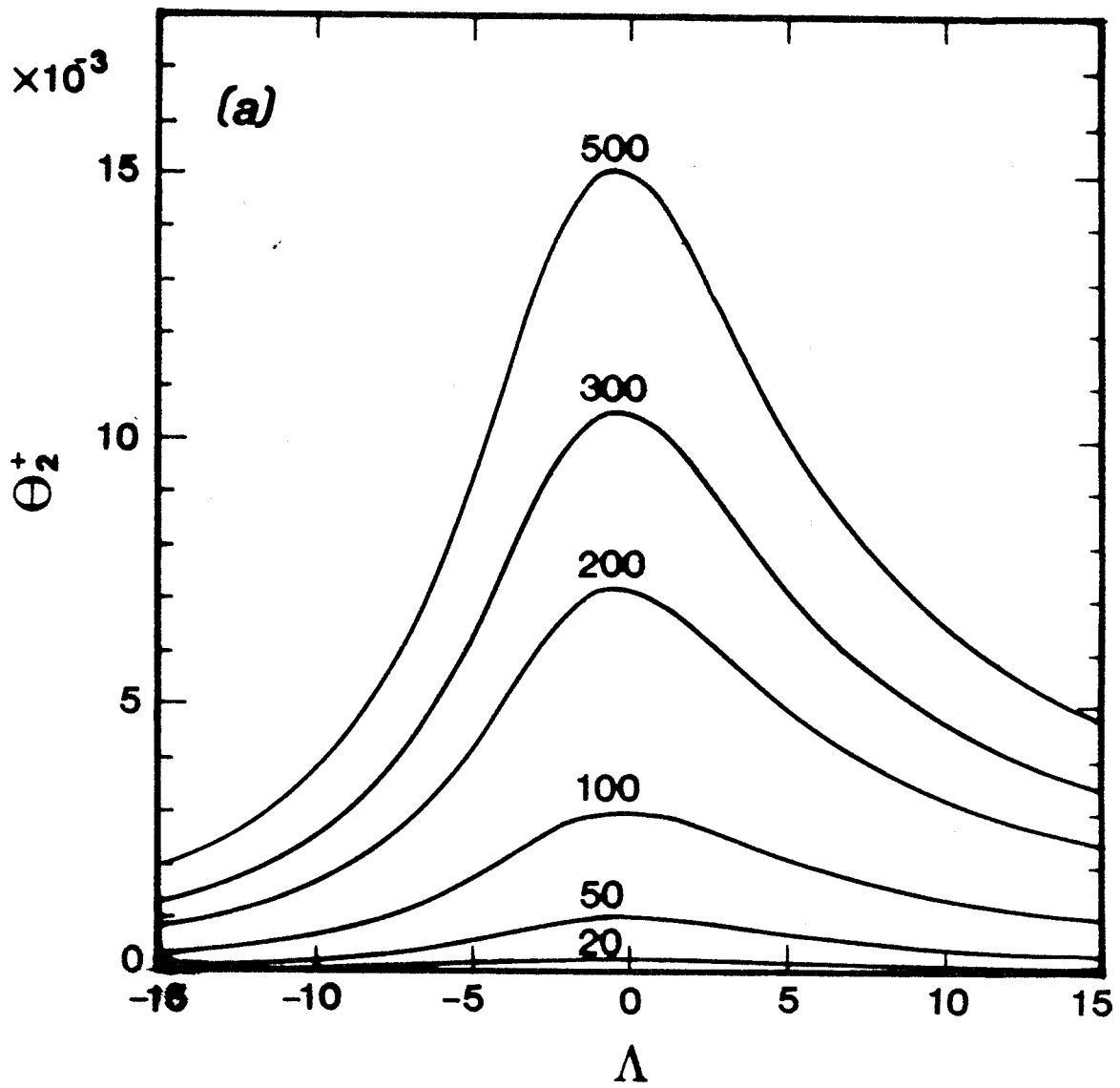


Figure 3 (a)

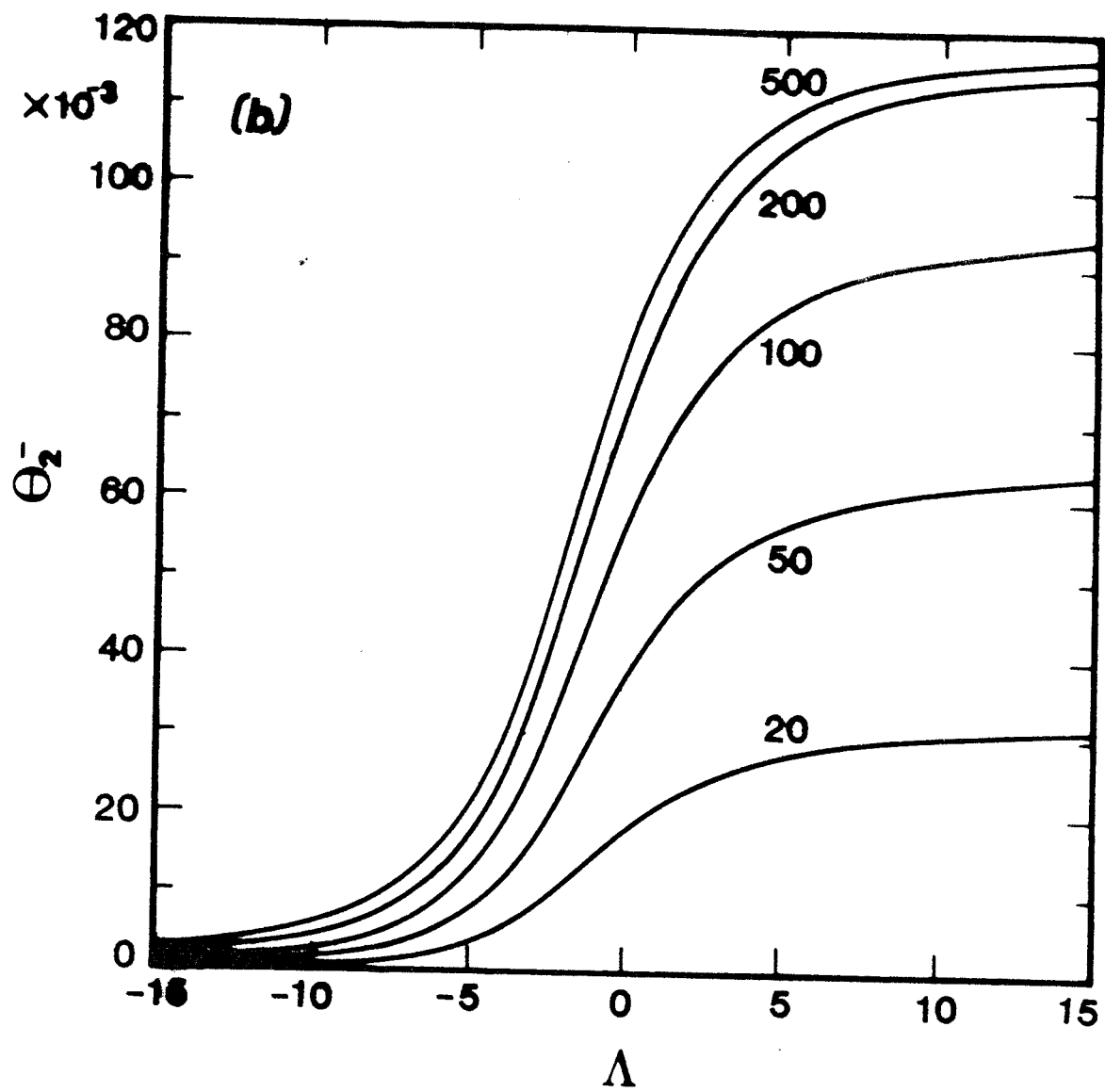


Figure 3 (b)

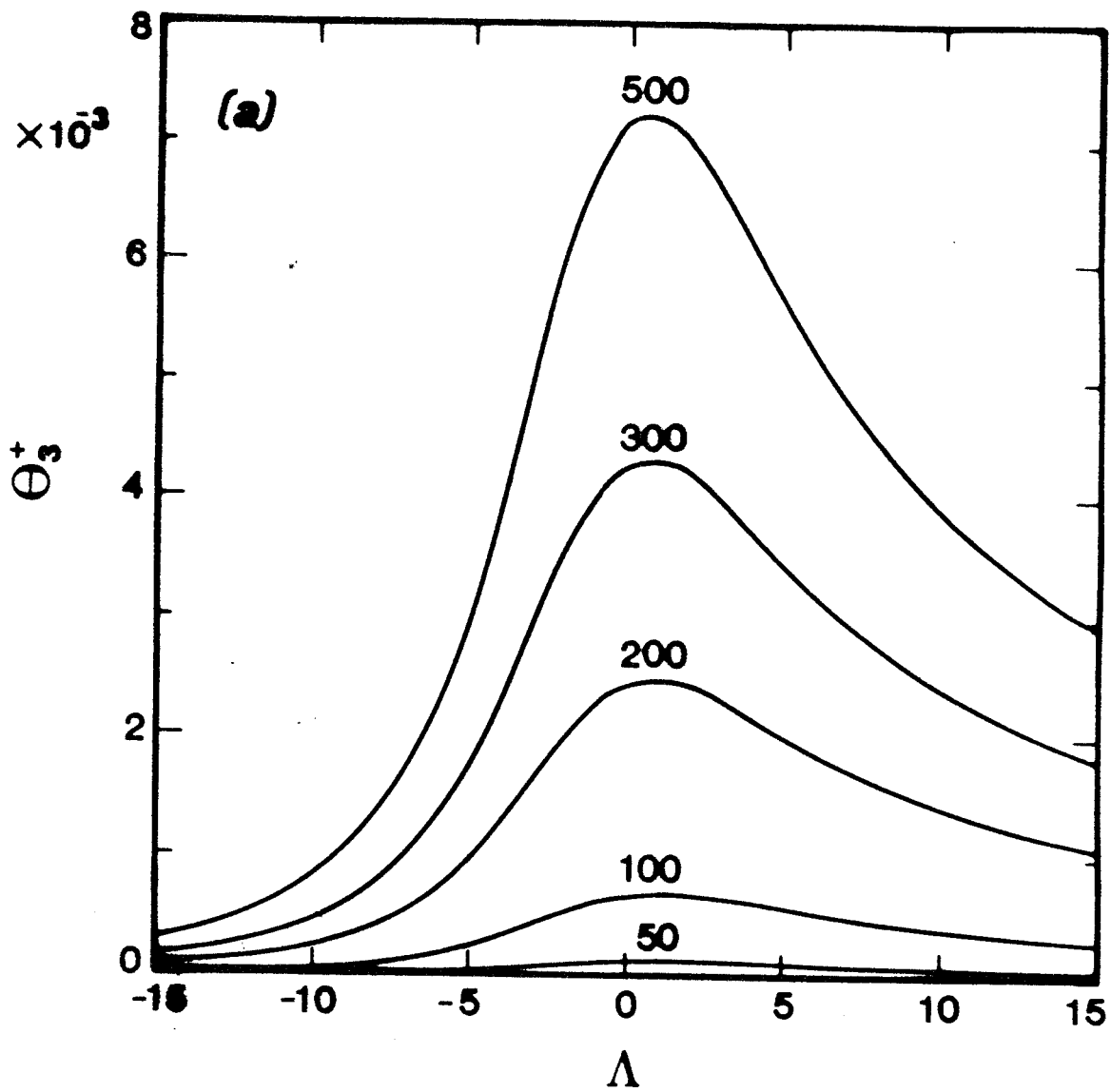


Figure 4 (a)

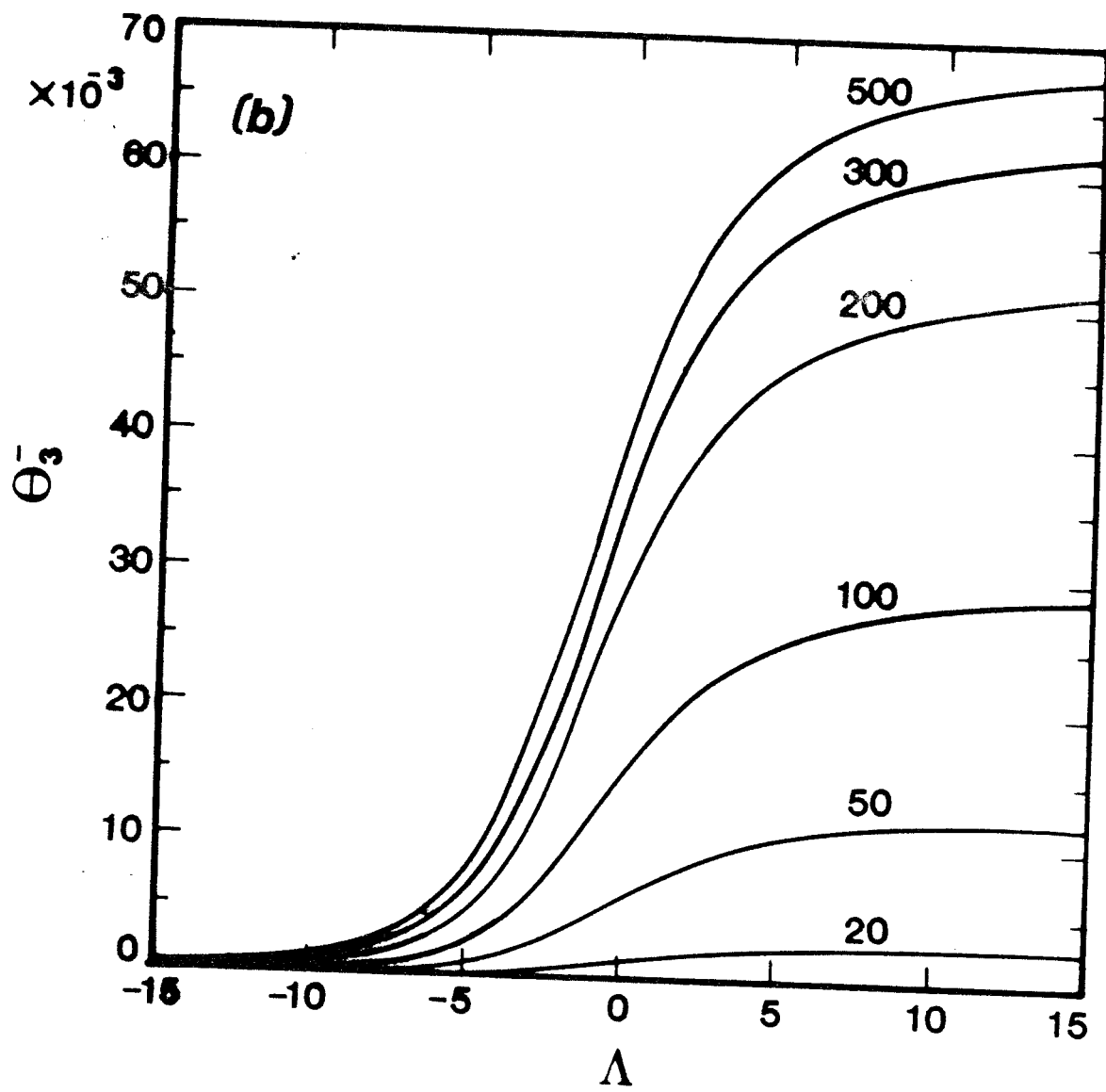


Figure 4 (b)

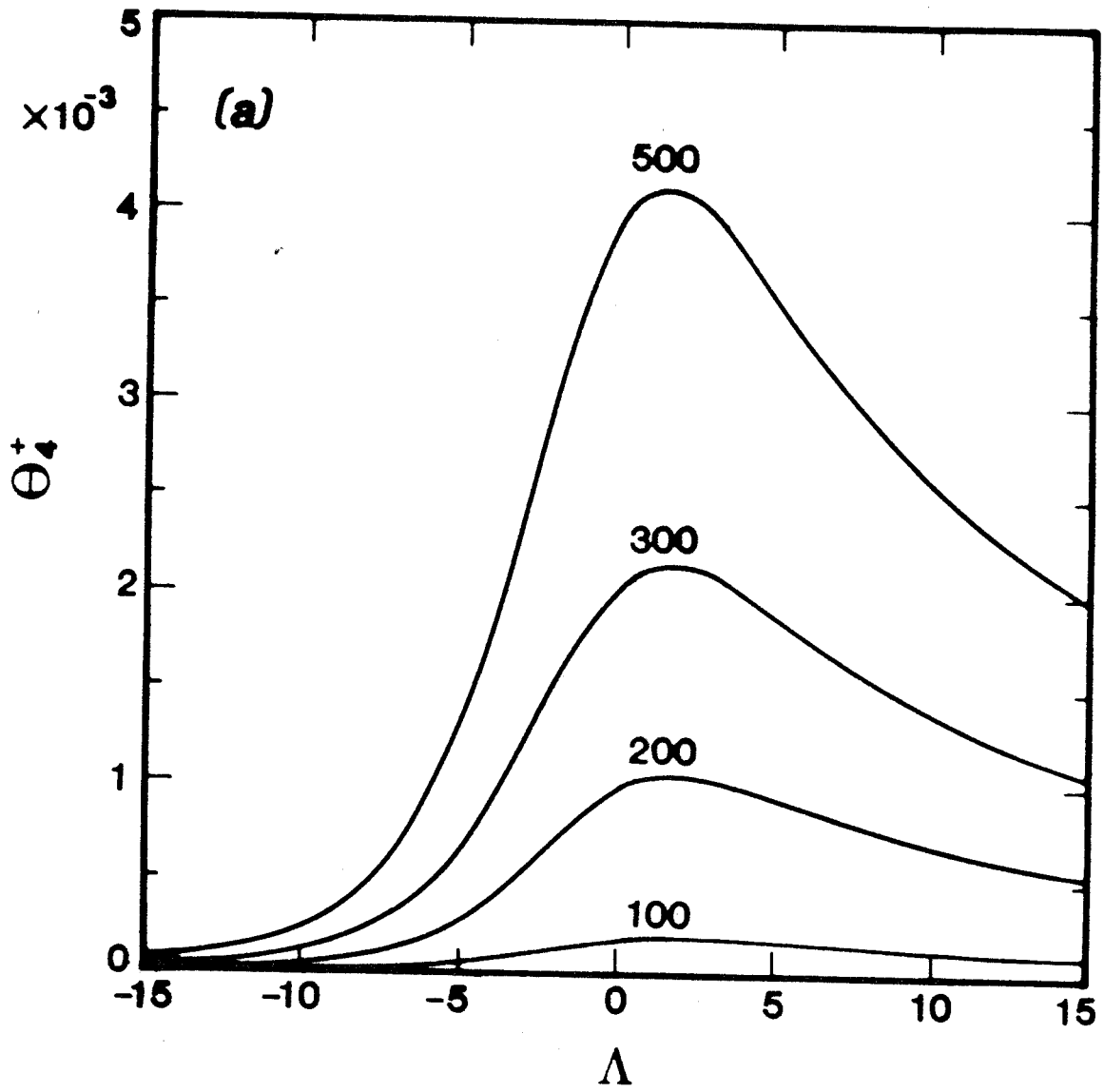


Figure 5 (a)

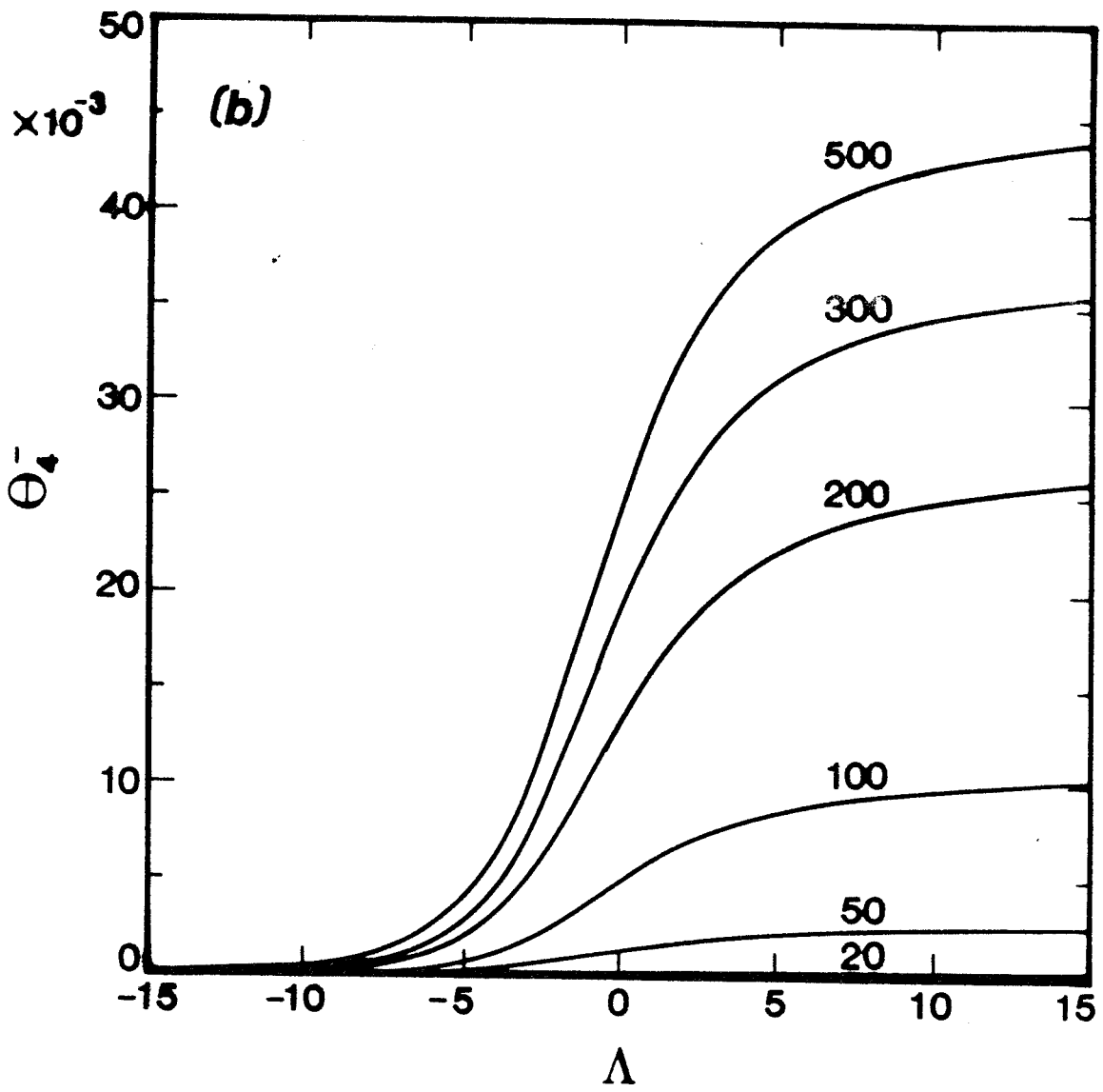


Figure 5 (b)

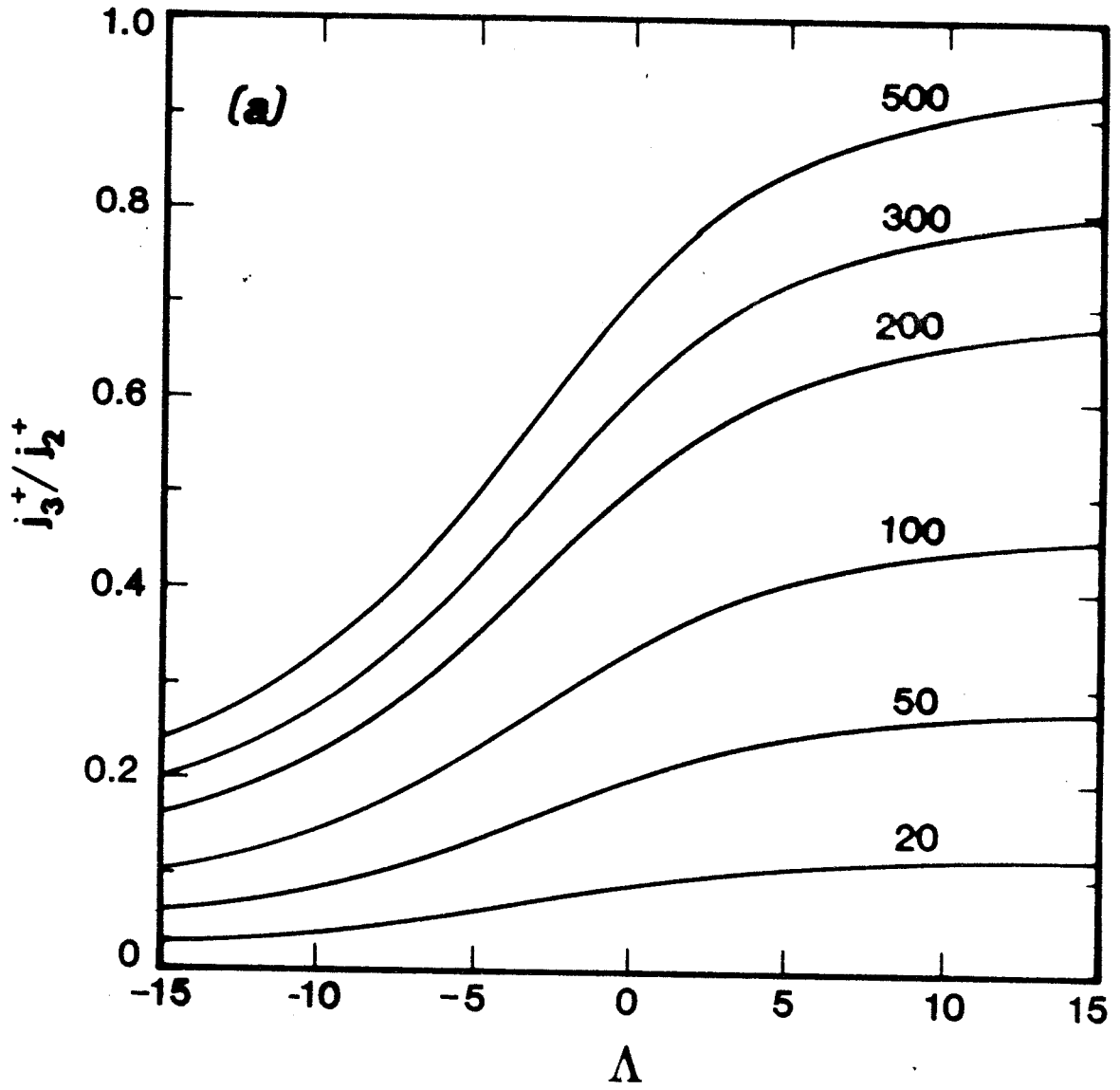


Figure 6 (a)

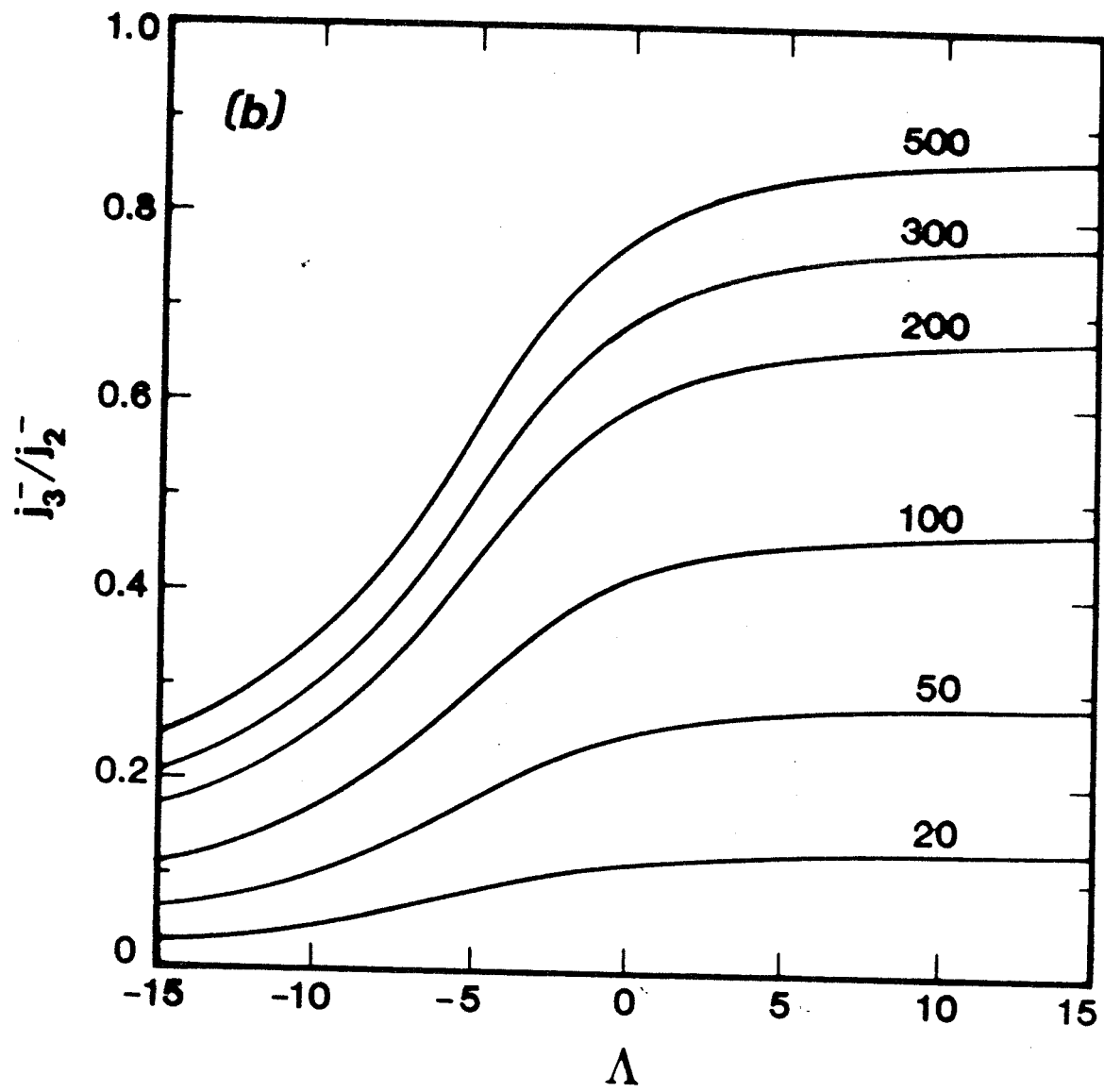


Figure 6 (b)

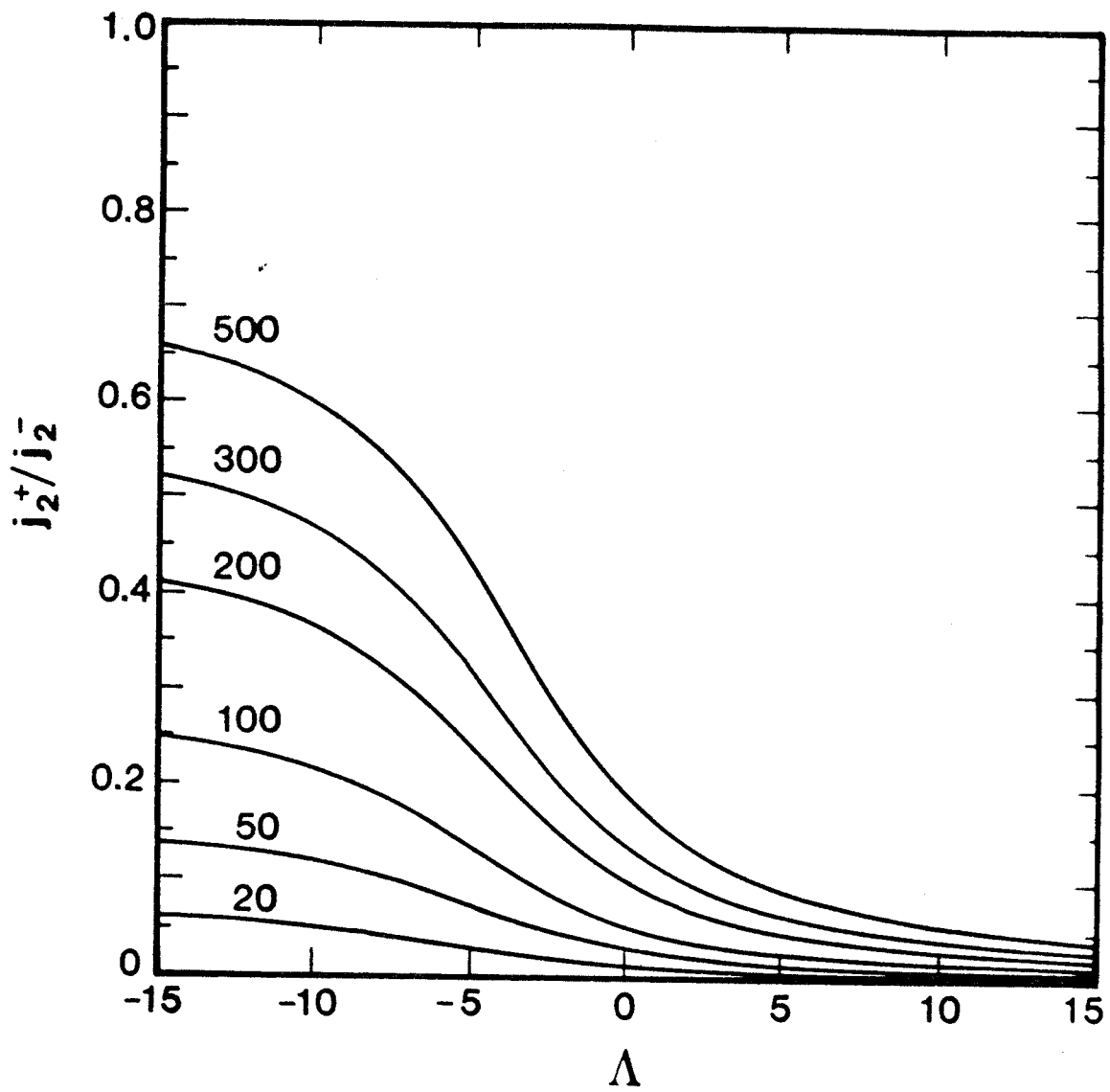


Figure 7.

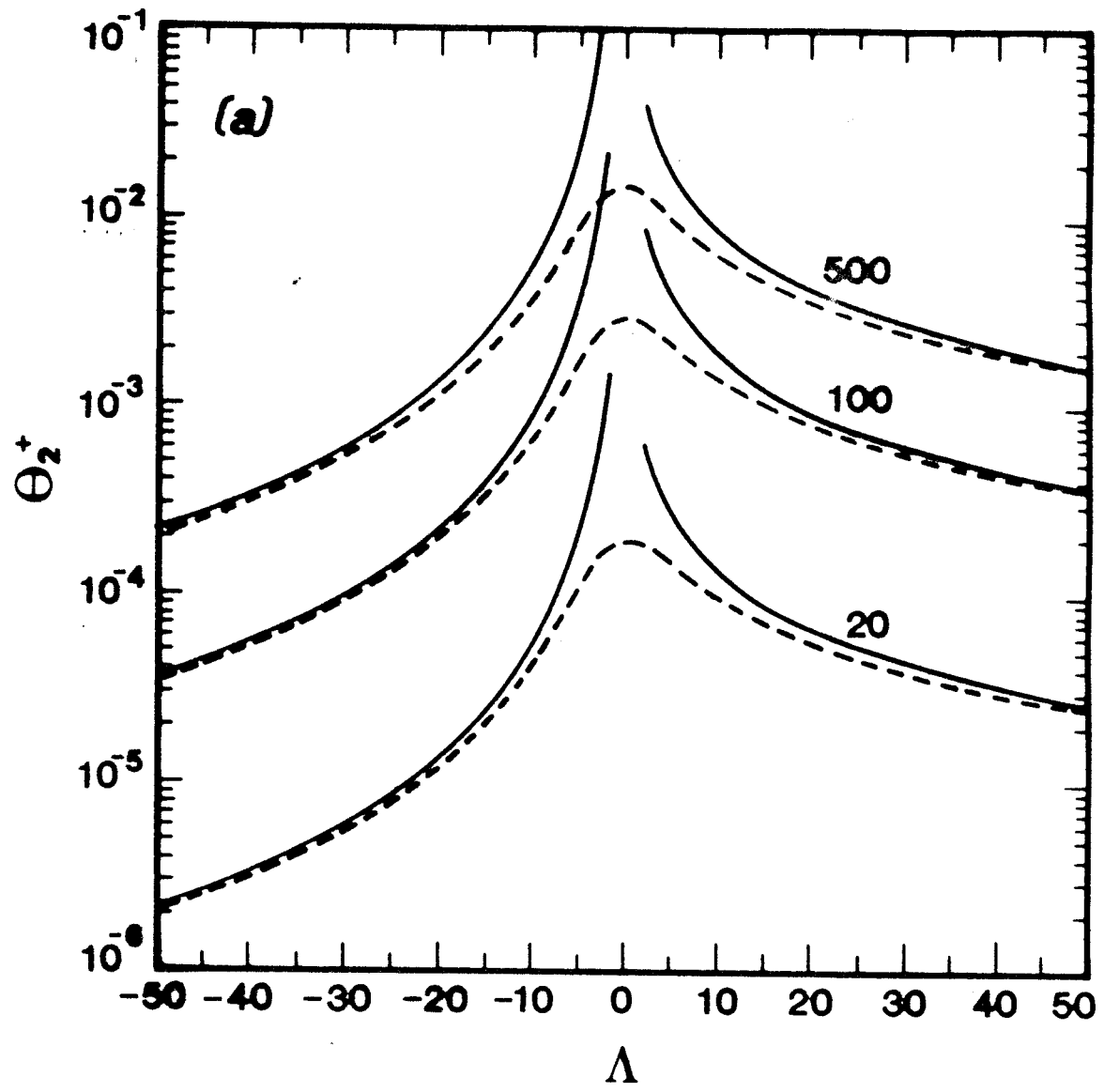


Figure 8 (a)

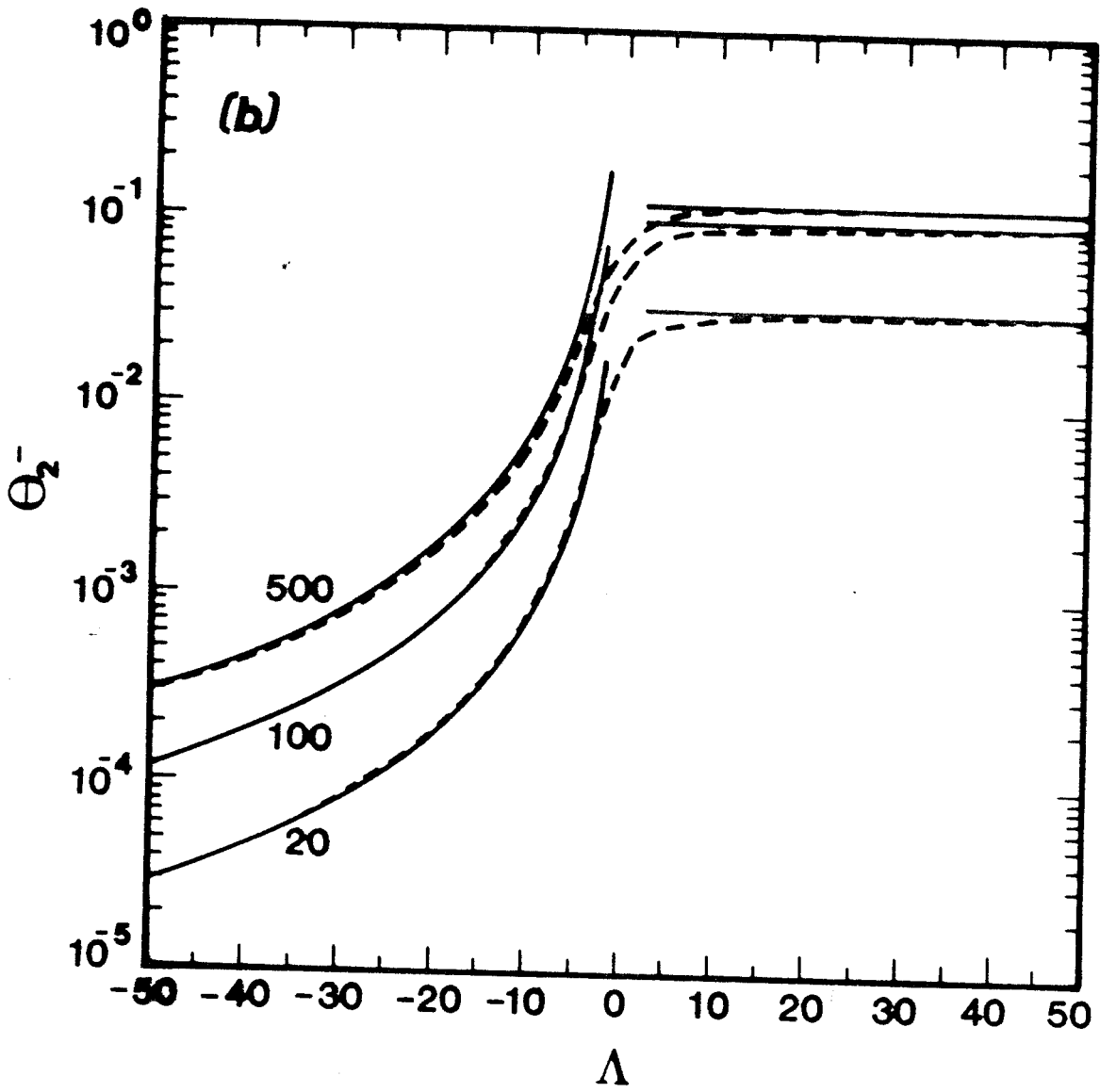


Figure 8 (b)

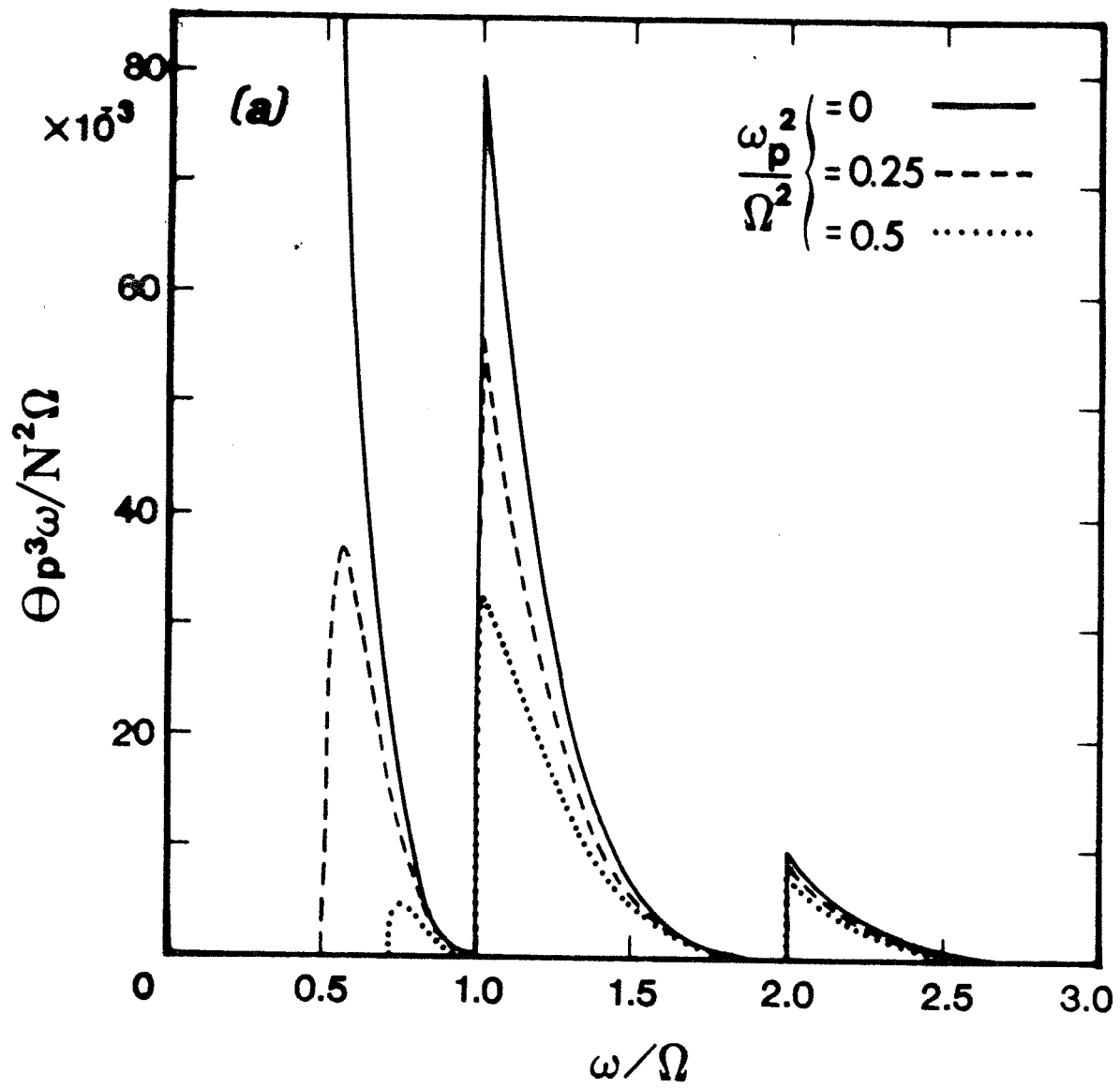


Figure 9 (a)

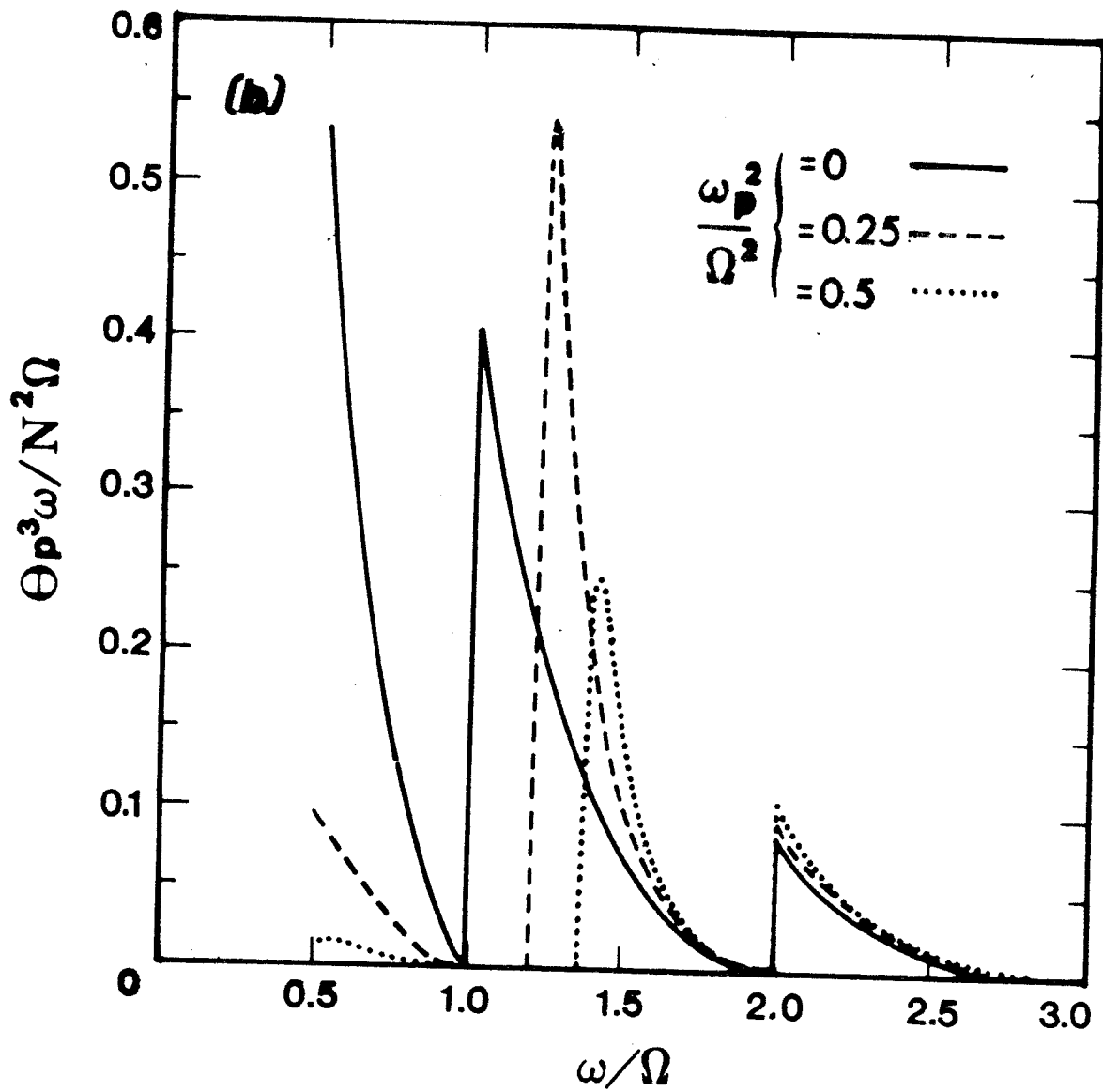


Figure 9 (b)